Y. Chen
Assistant Professor
School of Mechanical and Aerospace Engineering,
Nanyang Technological University,
Singapore 639798, Singapore

Z. You[1]
University Lecturer
Department of Engineering Science,
University of Oxford,
Oxford, OX1 3PJ, UK
e-mail: zhong.you@eng.ox.ac.uk

An Extended Myard Linkage and its Derived 6*R* Linkage

In this paper, a 6R linkage suitable as a building block for the construction of large deployable structures is presented. First, we report the possibility of construct an extended 5R Myard linkage by combining two complimentary Bennett linkages. Unlike the original 5R Myard linkage (also called Myard's "number 1" linkage), the angle of twists in the Bennett linkages is not necessary to be $\pi/2$. Then we show that a 6R linkage can be produced by merging two extended Myard linkages together and removing the common links. The closure equations for the 6R linkage are derived and its motion characteristics are discussed. Moreover, we demonstrate that a number of such 6R linkages can be assembled together to form a large-scale deployable structure, which opens to a flat profile. [DOI: 10.1115/1.2885506]

Keywords: Bennett linkage, Myard 5R linkage, 6R linkage, closure equation

1 Introduction

Overconstrained spatial closed-loop linkages have always drawn much research interest from kinematicians. In general, seven links, connected by revolute joints, are needed to form a mobile loop according to Kutzbach criterion [1]. All of the spatial 4*R*, 5*R*, and 6*R* closed-loop linkages are regarded as overconstrained simply because their mobility is due to special geometrical arrangements.

Since the publication of Bennett's famous paper "a new mechanism" [2], a number of 3D overconstrained closed-loop linkages have been found by combining or merging several Bennett linkages. Examples include the Myard linkages [3], the Goldberg 5*R* and 6*R* linkages [4], the Bennett-joint 6*R* linkage [5], the Dietmaier 6*R* linkage [6], and the Wohlhart double-Goldberg linkages [7] and most recently some 6*R* linkages by Chen [8] and Baker [9]. Baker [10,11] produced two excellent reviews of the existing Bennett-based 5*R* and 6*R* closed-loop linkages.

Closed-loop linkages were used in the past as deployable structures for aerospace applications. Examples such as deployable rims for space antennas and expandable solar array frames were reported by Gan and Pellegrino [12]. Even in the most common deployable structures consisting of scissorlike elements, 6*R* linkages such as the Sarrus linkage exist. Better understanding and selection of such mechanisms can be beneficial to design engineers.

In this paper, particular attention is paid to the Myard linkage, an overconstrained 5*R* linkage. It is a plane-symmetric 5*R* for which the two "rectangular" Bennett chains, with one pair of twists being $\pi/2$, are symmetrically disposed before combining them. The Bennett linkages are mirror images of each other, the mirror being coincident with the plane of symmetry of the resultant linkage [10]. Myard [3] applied this method to two rectangular Bennett linkages, resulting in his "number 1" 5*R* linkage.[2] We have found that under certain conditions, other Bennett linkages can also be combined together to obtain a 5*R* linkage with single degree of mobility using the similar method as Myard did. The conditions are that, first, the lengths of the links of one Bennett linkage must be equal to those of the respective links of the other Bennett linkage; secondly, one set of twists of the Bennett linkages are the same whereas the other sets are complimentary to each other. Unlike Myard's number 1 5*R* linkage, the new linkage does not have the symmetric plane. We call this the extended Myard linkage.

In a previous study, it has been found the Myard linkages can be used as deployable units for the construction of an umbrella-shape deployable structure [13]. Figure 1 shows such a structure consisting of seven Myard linkages arranged side by side. The neighboring linkages share a common link and the two joints at its ends. In this paper, we shall show that a better deployable unit can be obtained by combining two extended Myard linkages together to form a 6*R* linkage. This linkage can be used as a building block for the construction of large deployable frames.

The layout of this paper is as follows. First, in Sec. 2 we explain the way to build the extended Myard 5*R* linkage by combining two Bennett linkages. Then in Sec. 3, a detailed description of the construction of the 6*R* linkage is given, together with its closure equations and a discussion on its motion characteristics. Section 4 focuses on the use of the 6*R* linkage as a building block for large deployable structures. Some remarks on possible extension to the newly found 6*R* in Sec. 5 conclude the paper.

2 Extended Myard Linkage

Baker [10] gave the geometric condition and closure equations of the number 1 Myard linkage through the analysis of a Goldberg 5*R* linkage. So the Myard 5*R* linkage was treated as special case of the Goldberg 5*R* linkage. Here we treat the Myard linkage as the combination of two Bennett linkages as Myard did originally. Moreover, by following Myard's method, we have found that it is possible to obtain a linkage that we call the extended Myard linkage.

Consider two Bennett linkages shown in Fig. 2(*a*). The geometric parameters and closure equations of Bennett linkages **a** and **b** are

$$a_{12}^{\mathbf{m}} = a_{34}^{\mathbf{m}} = a^{\mathbf{m}}, \quad a_{23}^{\mathbf{m}} = a_{41}^{\mathbf{m}} = b^{\mathbf{m}} \tag{1a}$$

$$\alpha_{12}^{\mathbf{m}} = \alpha_{34}^{\mathbf{m}} = \alpha^{\mathbf{m}}, \quad \alpha_{23}^{\mathbf{m}} = \alpha_{41}^{\mathbf{m}} = \beta^{\mathbf{m}} \tag{1b}$$

$$\frac{\sin \alpha^{\mathbf{m}}}{a^{\mathbf{m}}} = \frac{\sin \beta^{\mathbf{m}}}{b^{\mathbf{m}}} \tag{1c}$$

and

$$\theta_1^{\mathbf{m}} + \theta_3^{\mathbf{m}} = 2\pi, \quad \theta_2^{\mathbf{m}} + \theta_4^{\mathbf{m}} = 2\pi \tag{2a}$$

[1]Corresponding author.
[2]This is the term used by Baker [10].

Contributed by the Mechanisms and Robotics Committee of ASME for publication in the JOURNAL OF MECHANICAL DESIGN. Manuscript received January 15, 2007; final manuscript received September 27, 2007; published online March 25, 2008. Review conducted by Ashitava Ghosal.

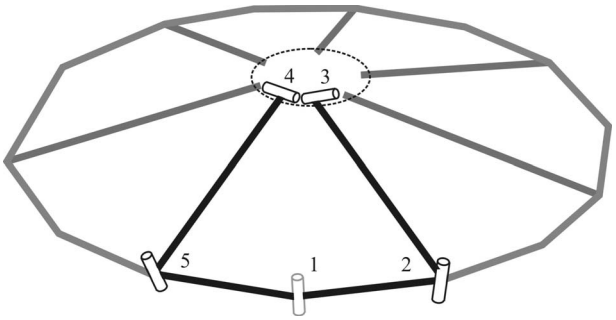

Fig. 1 A schematic diagram for an umbrellalike deployable frame made from seven Myard linkages. Only one of the Myard linkages is highlighted.

$$\tan\frac{\theta_1^{\mathbf{m}}}{2}\tan\frac{\theta_2^{\mathbf{m}}}{2}=\frac{\sin\frac{1}{2}(\alpha_{23}^{\mathbf{m}}+\alpha_{12}^{\mathbf{m}})}{\sin\frac{1}{2}(\alpha_{23}^{\mathbf{m}}-\alpha_{12}^{\mathbf{m}})}=\frac{\sin\frac{1}{2}(\beta^{\mathbf{m}}+\alpha^{\mathbf{m}})}{\sin\frac{1}{2}(\beta^{\mathbf{m}}-\alpha^{\mathbf{m}})}=K^{\mathbf{m}} \tag{2b}$$

where $\mathbf{m}=\mathbf{a}$ or $\mathbf{b}$.

Similar to Myard's approach, Bennett linkages **a** and **b** are combined together by fixing Links 34 and 41 of **a** with Links 12 and 41 of **b**, respectively, and Joints 3 and 4 of **a** and Joints 2 and 1 of **b** become collinear, respectively, see Fig. 2(*b*). In order to obtain such connection, the following conditions must be satisfied:

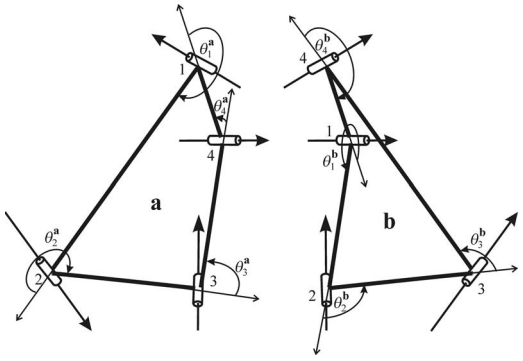

(*a*)

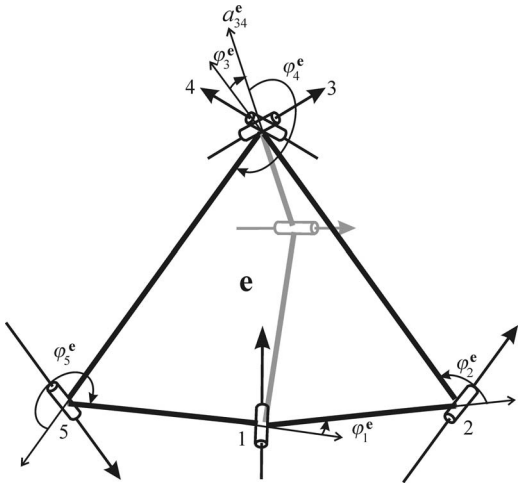

(*b*)

Fig. 2 (*a*) Two Bennett linkages a and b. (*b*) They are combined to form an extended Myard linkage e.

(a) $a_{34}^{\mathbf{a}}=a_{12}^{\mathbf{b}}$ or $a^{\mathbf{a}}=a^{\mathbf{b}}=a$

(b) $a_{41}^{\mathbf{a}}=a_{41}^{\mathbf{b}}$ or $b^{\mathbf{a}}=b^{\mathbf{b}}=b$

(c) $\alpha_{34}^{\mathbf{a}}=\alpha_{12}^{\mathbf{b}}$ or $\alpha^{\mathbf{a}}=\alpha^{\mathbf{b}}=\alpha$ and

(d) $\sin\beta^{\mathbf{a}}=\sin\beta^{\mathbf{b}}$ because of Eq. (1*c*)

There are two solutions to the last condition:

$$\beta^{\mathbf{a}}=\beta^{\mathbf{b}}\ \text{or}\ \beta^{\mathbf{a}}+\beta^{\mathbf{b}}=\pi$$

The first solution leads to the formation of a single Bennett linkage, which is not what we intended to, whereas the second solution forms a 5*R* linkage **e** should the two common links and the joint connecting them, shown in gray color in Fig. 2(*b*), be removed. The conditions that the geometric parameters of the newly formed 5*R* linkage ought to satisfy are as follows:

$$a_{34}^{\mathbf{e}}=0,\quad a_{12}^{\mathbf{e}}=a_{51}^{\mathbf{e}}=b,\quad a_{23}^{\mathbf{e}}=a_{45}^{\mathbf{e}}=a \tag{3a}$$

$$\alpha_{23}^{\mathbf{e}}=\alpha_{45}^{\mathbf{e}}=\alpha,\quad \alpha_{51}^{\mathbf{e}}=\beta,\quad \alpha_{12}^{\mathbf{e}}=\pi-\beta,\quad \alpha_{34}^{\mathbf{e}}=\alpha_{51}^{\mathbf{e}}-\alpha_{12}^{\mathbf{e}}=2\beta-\pi \tag{3b}$$

$$R_i^{\mathbf{e}}=0\quad (i=1,2,\ldots,5) \tag{3c}$$

and

$$\frac{\sin\alpha}{a}=\frac{\sin\beta}{b} \tag{3d}$$

The relationships among the revolute variables of this 5*R* linkage **e** and the Bennett linkages **a** and **b** are as follows:

$$\varphi_1^{\mathbf{e}}+\pi=\theta_3^{\mathbf{a}}+\theta_2^{\mathbf{b}} \tag{4a}$$

$$\varphi_2^{\mathbf{e}}=\theta_3^{\mathbf{b}} \tag{4b}$$

$$\varphi_3^{\mathbf{e}}=\theta_4^{\mathbf{b}}-\pi \tag{4c}$$

$$\varphi_4^{\mathbf{e}}=\theta_1^{\mathbf{a}} \tag{4d}$$

$$\varphi_5^{\mathbf{e}}=\theta_2^{\mathbf{a}} \tag{4e}$$

From Eqs. (2*a*) and (4*a*), we can obtain that

$$\varphi_1^{\mathbf{e}}+\varphi_3^{\mathbf{e}}+\varphi_4^{\mathbf{e}}=2\pi \tag{5a}$$

Because $\theta_1^{\mathbf{b}}+\theta_4^{\mathbf{a}}=2\pi$, and by considering Eq. (2*a*), we have

$$\varphi_2^{\mathbf{e}}+\varphi_5^{\mathbf{e}}=2\pi \tag{5b}$$

Because of Eq. (2*b*),

$$\tan\frac{\varphi_4^{\mathbf{e}}}{2}\tan\frac{\varphi_5^{\mathbf{e}}}{2}=K^{\mathbf{a}} \tag{5c}$$

and

$$\tan\frac{\pi+\varphi_3^{\mathbf{e}}}{2}\tan\frac{\varphi_2^{\mathbf{e}}}{2}=K^{\mathbf{b}}$$

i.e.,

$$\tan\frac{\varphi_2^{\mathbf{e}}}{2}=-K^{\mathbf{b}}\tan\frac{\varphi_3^{\mathbf{e}}}{2} \tag{5d}$$

From Eqs. (5*b*)–(5*d*), we can obtain that

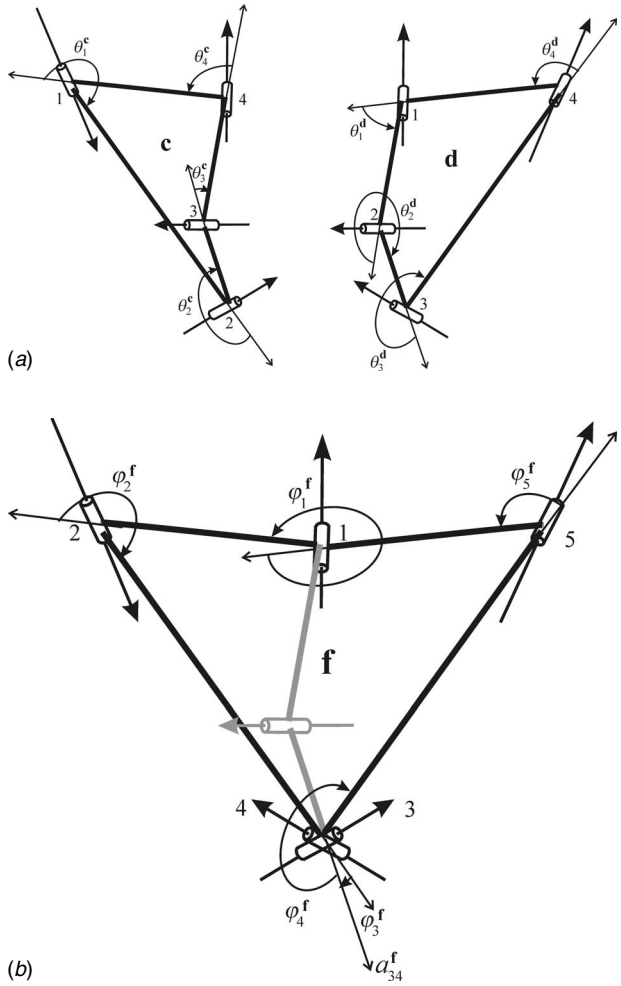

Fig. 3 (*a*) Two Bennett linkages c and d. (*b*) They are combined to form an extended Myard linkage f.

$$\tan\frac{\varphi_3^{\mathbf{e}}}{2}\tan\frac{\varphi_4^{\mathbf{e}}}{2}=\frac{K^{\mathbf{a}}}{K^{\mathbf{b}}} \tag{5e}$$

So Eqs. (5*a*)–(5*d*) are the closure equations of extended Myard linkage **e**. This linkage has only one degree of mobility based on the equations.

In Bennett linkage **a**, if Link 23 is fixed and Link 34 is rotated to a position below Link 23, the linkage change from the configuration in Fig. 2(*a*) to the configuration in Fig. 3(*a*), and in this case, let us name it as Bennett linkage **c**. Applying the same operation to Bennett linkage **b** yields Bennett linkage **d** in Fig. 3(*a*). Under such configurations, Bennett linkages **c** and **d** can be combined together to form the other extended Myard linkage **f** by removing the common links and joint as shown in Fig. 3(*b*). The conditions on its geometric parameters are as follows:

$$a_{34}^{\mathbf{f}}=0,\quad a_{12}^{\mathbf{f}}=a_{51}^{\mathbf{f}}=b,\quad a_{23}^{\mathbf{f}}=a_{45}^{\mathbf{f}}=a \tag{6a}$$

$$\alpha_{23}^{\mathbf{f}}=\alpha_{45}^{\mathbf{f}}=\alpha,\quad \alpha_{12}^{\mathbf{f}}=\beta,\quad \alpha_{51}^{\mathbf{f}}=\pi-\beta,\quad \alpha_{34}^{\mathbf{f}}=\alpha_{51}^{\mathbf{f}}-\alpha_{12}^{\mathbf{f}}=\pi-2\beta \tag{6b}$$

$$R_i^{\mathbf{f}}=0\quad (i=1,2,\ldots,5) \tag{6c}$$

and

$$\frac{\sin\alpha}{a}=\frac{\sin\beta}{b} \tag{6d}$$

The relationship among the revolute variables between linkages **f**, **c**, and **d** is as follows:

$$2\pi-\varphi_1^{\mathbf{f}}=\pi-\theta_1^{\mathbf{d}}-\theta_4^{\mathbf{c}} \tag{7a}$$

$$\varphi_2^{\mathbf{f}}=\theta_1^{\mathbf{c}} \tag{7b}$$

$$\varphi_3^{\mathbf{f}}=\theta_2^{\mathbf{c}}-\pi \tag{7c}$$

$$\varphi_4^{\mathbf{f}}=\theta_3^{\mathbf{d}} \tag{7d}$$

$$\varphi_5^{\mathbf{f}}=\theta_4^{\mathbf{d}} \tag{7e}$$

From Eqs. (7*a*) and (2*a*), we can obtain that

$$\varphi_1^{\mathbf{f}}+\varphi_3^{\mathbf{f}}+\varphi_4^{\mathbf{f}}=4\pi \tag{8a}$$

Because $\theta_3^{\mathbf{c}}+\theta_2^{\mathbf{d}}=2\pi$, we have

$$\varphi_2^{\mathbf{f}}+\varphi_5^{\mathbf{f}}=2\pi \tag{8b}$$

and

$$\tan\frac{\varphi_5^{\mathbf{f}}}{2}\tan\frac{\varphi_4^{\mathbf{f}}}{2}=K^{\mathbf{b}} \tag{8c}$$

$$\tan\frac{\varphi_2^{\mathbf{f}}}{2}=-K^{\mathbf{a}}\tan\frac{\varphi_3^{\mathbf{f}}}{2} \tag{8d}$$

From Eqs. (8*b*) and (8*d*), we can obtain that

$$\tan\frac{\varphi_3^{\mathbf{f}}}{2}\tan\frac{\varphi_4^{\mathbf{f}}}{2}=\frac{K^{\mathbf{b}}}{K^{\mathbf{a}}} \tag{8e}$$

So Eqs. (8*a*)–(8*d*) are the closure equations of extended Myard linkage **f**. Again this linkage has only one degree of mobility.

Comparing the result of the extended Myard linkages **e** and **f**, we can obtain that geometric parameters of a common extended Myard 5*R* linkage should satisfy that

$$a_{34}=0,\quad a_{12}=a_{51},\quad a_{23}=a_{45} \tag{9a}$$

$$\alpha_{23}=\alpha_{45},\quad \alpha_{51}=\pi-\alpha_{12},\quad \alpha_{34}=\pi-2\alpha_{12} \tag{9b}$$

$$R_i=0\quad (i=1,2,\ldots,5) \tag{9c}$$

and

$$\frac{\sin\alpha_{12}}{a_{12}}=\frac{\sin\alpha_{23}}{a_{23}} \tag{9d}$$

Moreover, the closure equations are

$$\varphi_1+\varphi_3+\varphi_4=2n\pi\quad (n=1\text{ or }2) \tag{10a}$$

$$\varphi_2+\varphi_5=2\pi \tag{10b}$$

$$\tan\frac{\varphi_4}{2}\tan\frac{\varphi_5}{2}=\frac{\sin\frac{1}{2}(\pi-\alpha_{12}+\alpha_{23})}{\sin\frac{1}{2}(\pi-\alpha_{12}-\alpha_{23})} \tag{10c}$$

and

$$\tan\frac{\varphi_2}{2}=-\frac{\sin\frac{1}{2}(\alpha_{12}+\alpha_{23})}{\sin\frac{1}{2}(\alpha_{12}-\alpha_{23})}\tan\frac{\varphi_3}{2} \tag{10d}$$

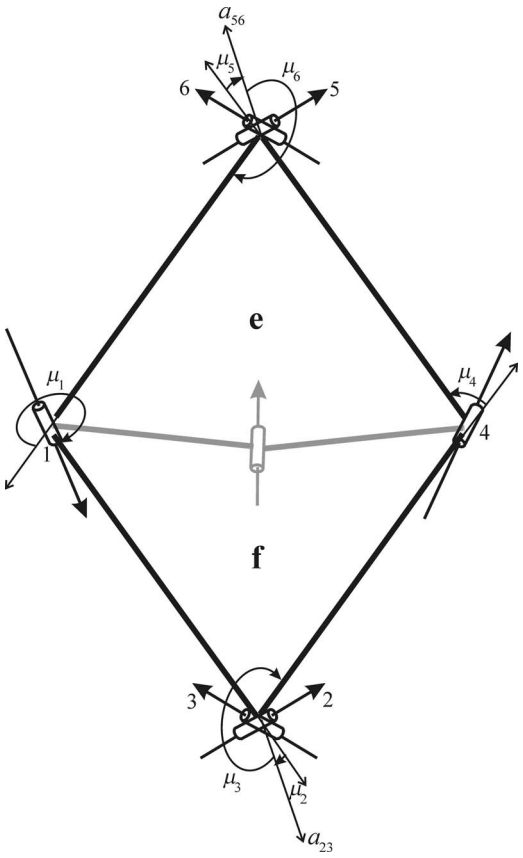

Fig. 4 A 6*R* linkage from two extended Myard linkages e and f

Note that the difference between the number 1 Myard linkage and the extended Myard linkage is that the former requires a pair of twists being set as $\pi/2$, whereas such requirement is unnecessary for the latter.

3 6*R* Linkage

3.1 Construction. Wholhart [7] created a novel 6*R* linkage by hybridization of two number 1 Myard 5*R* linkages. The same can be applied to a pair of the extended Myard linkages.

If we combine extended Myard linkages **e** and **f** together by fixing Links 51 and 12 of **e** with Links 12 and 51 of **f**, respectively, and merging Joints 5, 1, and 2 of **e** with Joints 2, 1, and 5 of **f**, respectively, into three joints, then a 6*R* linkage is formed by removing the common links and Joint 1, see Fig. 4.

3.2 Closure Equations. The conditions on the geometric parameters of the newly formed linkage are

$$a_{12} = a_{34} = a_{45} = a_{61}, \quad a_{23} = a_{56} = 0 \tag{11a}$$

$$\alpha_{12} = \alpha_{34} = \alpha_{45} = \alpha_{61}, \quad \alpha_{23} + \alpha_{56} = 2\pi \tag{11b}$$

$$R_i = 0, \quad (i = 1,2, \ldots 6) \tag{11c}$$

The relationships among the revolute variables of this 6*R* linkage and those of linkages **e** and **f** are as follows:

$$\mu_1 + \pi = \varphi_5^{\mathbf{e}} + \varphi_2^{\mathbf{f}} \tag{12a}$$

$$\mu_2 = \varphi_3^{\mathbf{f}} \tag{12b}$$

$$\mu_3 = \varphi_4^{\mathbf{f}} \tag{12c}$$

$$\mu_4 + \pi = \varphi_2^{\mathbf{e}} + \varphi_5^{\mathbf{f}} \tag{12d}$$

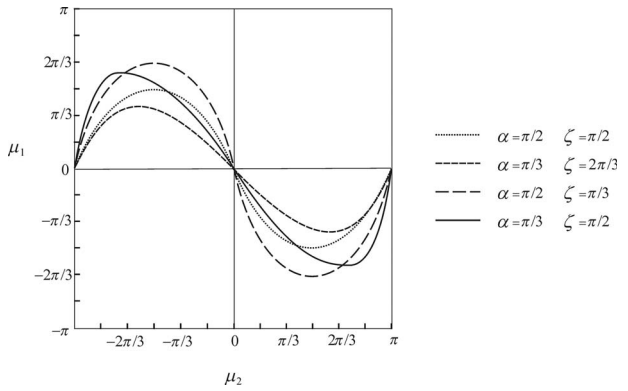

Fig. 5 μ_1 versus μ_2 for 6*R* linkage

$$\mu_5 = \varphi_3^{\mathbf{e}} \tag{12e}$$

$$\mu_6 = \varphi_4^{\mathbf{e}} \tag{12f}$$

From Eq. (5*e*), there is

$$\tan\frac{\mu_5}{2}\tan\frac{\mu_6}{2} = \frac{K^{\mathbf{a}}}{K^{\mathbf{b}}} \tag{13}$$

From Eq. (8*e*), we have

$$\tan\frac{\mu_2}{2}\tan\frac{\mu_3}{2} = \frac{K^{\mathbf{b}}}{K^{\mathbf{a}}} = \frac{1+\tan\alpha_{12}\tan\dfrac{\alpha_{56}}{2}}{1-\tan\alpha_{12}\tan\dfrac{\alpha_{56}}{2}} \tag{14a}$$

Based on Eqs. (5*b*), (8*b*), (12*a*), and (12*d*), it is obtained that

$$\mu_1 + \mu_4 = 2\pi \tag{14b}$$

Now consider Eqs. (12*b*) and (12*e*). Owing to Eqs. (5*a*) and (8*a*), we can obtain that

$$\mu_2 + \mu_5 = 6\pi - \varphi_1^{\mathbf{e}} - \varphi_1^{\mathbf{f}} - \varphi_4^{\mathbf{e}} - \varphi_4^{\mathbf{f}}$$

Since $\varphi_1^{\mathbf{e}} + \varphi_1^{\mathbf{f}} = 2\pi$ and $\varphi_4^{\mathbf{e}} + \varphi_4^{\mathbf{f}} = 3\pi$, there is

$$\mu_2 + \mu_5 = \pi \tag{14c}$$

From Eqs. (13), (14*a*), and (14*c*), we have

$$\mu_3 + \mu_6 = 3\pi \tag{14d}$$

Finally, from Eq. (12*a*),

$$\tan\frac{\mu_1+\pi}{2} = \tan\frac{\varphi_5^{\mathbf{e}} + \varphi_2^{\mathbf{f}}}{2}$$

Considering Eqs. (5*c*) and (8*d*), we can derive that

$$\tan\frac{\mu_1}{2} = -\frac{\sin\mu_2}{\sin\alpha_{12}\tan\dfrac{\alpha_{56}}{2} + \cos\alpha_{12}\cos\mu_2} \tag{14e}$$

Equations (14*a*)–(14*e*) are the closure equations of the new 6*R* linkage. The linkage has only a single degree of mobility in general.

3.3 Deployment Properties. The relationship between the revolute variables μ_1 and μ_2 for the new 6*R* linkage is given in Eq. (14*e*). For a set of given $\alpha_{12}=\alpha$ and $\alpha_{56}=\zeta$, μ_1 versus μ_2 curves are plotted in Fig. 5. It is interesting to note that all of the curves pass points (0, 0) and (π,0), which suggests that there is a common configuration that four non-zero-length links can become colinear. Moreover, the maximum value for μ_1 is reached when μ_2 changes from 0 to π, which represents a configuration that four non-zero-length links form a rhombus. Particularly when α_{12}

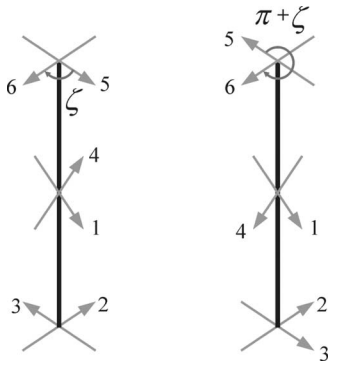

Fig. 6 The 6*R* linkages (*a*) for a given $\alpha_{56}=\zeta$ and (*b*) when α_{56} is increased to $\pi+\zeta$

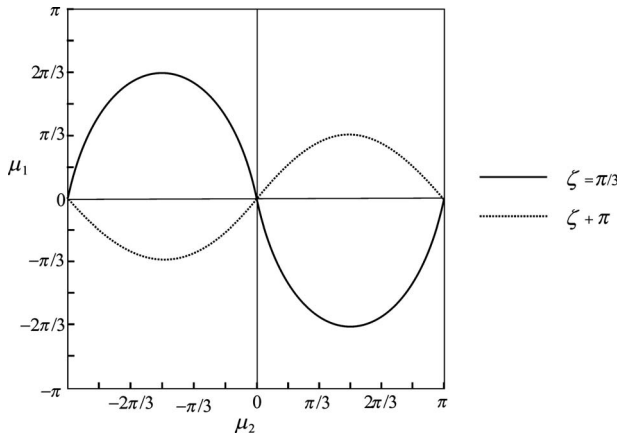

Fig. 7 μ_2 versus μ_1 for 6*R* linkages with a given $\alpha_{56}=\zeta$ and the other one when α_{56} is increased to $\pi+\zeta$

$=\alpha_{56}=\pi/2$, the rhombus becomes a square. All of these characteristics show that this new 6*R* linkage has a very compact folded state, as well as a state corresponding to the maximum expansion, which make it ideal as a deployable unit.

In general, the linkage has a single degree of freedom as indicated by the closure equations. However, the degree of freedom increases in some particular configurations. These configurations are best identified by calculating the state of self-stress of the linkage [14,15] as we did previously with another 6*R* linkage [16]. The analysis confirms that one state of self-stress exists at normal configurations, which corresponds to a single degree of mobility, and there are two states of self-stress at the configurations where $\mu_1=\mu_2=0$ and $\mu_1=0$, $\mu_2=\pi$, which implies that at these configurations bifurcation occurs.

Due to their similarity, only the configuration where $\mu_1=0$ and $\mu_2=\pi$ is discussed here. Figure 6(*a*) shows a 6*R* linkage, **g**, with given $\alpha_{12}=\alpha$ and $\alpha_{56}=\zeta$ when $\mu_1=0$ and $\mu_2=\pi$. Links 61 and 45 are now collinear. So are Links 12 and 34. The closure equations of this linkage are given in Eq. (14*a*)–(14*e*). Meanwhile, consider the other 6*R* linkage, **h**, where α_{12} remains the same as the previous one but α_{56} is increased by π. When $\mu_1=0$ and $\mu_2=\pi$, it looks rather similar to the previous linkage, see Fig. 6(*b*). The only difference between the two is that the orientation of Joints 3, 4, and 5 are opposite to each other, respectively. The relationships among the kinematic variables of two linkages are

$$\mu_1^{\mathbf{g}}=\mu_1^{\mathbf{h}},\quad \mu_2^{\mathbf{g}}=\mu_2^{\mathbf{h}},\quad \mu_6^{\mathbf{g}}=\mu_6^{\mathbf{h}}$$

and

$$\mu_3^{\mathbf{g}}+\mu_3^{\mathbf{h}}=2\pi,\quad \mu_4^{\mathbf{g}}+\mu_4^{\mathbf{h}}=2\pi,\quad \mu_5^{\mathbf{g}}+\mu_5^{\mathbf{h}}=2\pi$$

From Eq. (14*a*)–(14*e*), the closure equations for the second 6*R* linkage **h**, in which α_{12} remains α whereas α_{56} is increased from ζ to $\pi+\zeta$, are

$$\mu_4^{\mathbf{h}}=\mu_1^{\mathbf{h}} \tag{15a}$$

$$\mu_5^{\mathbf{h}}=\pi+\mu_2^{\mathbf{h}} \tag{15b}$$

$$\mu_6^{\mathbf{h}}=\pi+\mu_3^{\mathbf{h}} \tag{15c}$$

$$\tan\frac{\mu_2^{\mathbf{h}}}{2}\tan\frac{\mu_3^{\mathbf{h}}}{2}=\frac{\tan\alpha-\tan\dfrac{\zeta}{2}}{\tan\alpha+\tan\dfrac{\zeta}{2}} \tag{15d}$$

$$\tan\frac{\mu_1^{\mathbf{h}}}{2}=\frac{\sin\mu_2^{\mathbf{h}}\tan\dfrac{\zeta}{2}}{\sin\alpha-\cos\alpha\tan\dfrac{\zeta}{2}\cos\mu_2^{\mathbf{h}}} \tag{15e}$$

Figure 7 shows the μ_2 versus μ_1 curves based on Eqs. (14*e*) and (15*e*) for the 6*R* linkages with $\alpha_{12}=\pi/2$, $\alpha_{56}=\pi/3$ and $\alpha_{12}=\pi/2$, $\alpha_{56}=4\pi/3$, respectively. It clearly shows that when $\mu_1=\mu_2=0$ and $\mu_1=0$, $\mu_2=\pi$ the motion bifurcation could happen. The bifurcations can be demonstrated using a model shown in Fig. 8, which was built with the twists $\alpha_{12}=\pi/2$ and $\alpha_{56}=3\pi/2$. Figure 8(*a*) is the configuration corresponding to $\mu_1=\pi/2$, $\mu_2=\pi/2$. In Fig. 8(*b*), μ_1 is close to 0 and μ_2 to 0. At $\mu_1=\mu_2=0$, the linkage can move to either of the configurations shown in Figs. 8(*c*) and 8(*d*).

4 Assembly of the 6*R* Linkages

Using the 6*R* linkage, it is possible to construct a large-scale deployable assembly by connecting many of them according to the scheme shown in Fig. 9. A straight line section represents a single continuous member and each of the black squares, regardless of being large or small, represents a single 6*R* linkage. The small solid circle indicates a connection, such as Connections 2, 3 and 5, 6 in Fig. 4, where a zero length link is present, and the hollow circle denotes a simple pin connection. The solid circles are aligned to form a set of gray guidelines, whereas the hollow circles can also be aligned to form the other set of broken gray guidelines. During the deployment, both solid and broken gray guidelines are always straight and perpendicular to each other. All of the large and small 6*R* linkages on the whole assembly should have the same twists. The whole structure can be deployed to produce a flat profile and each of large or small 6*R* linkages is in a rhombus. When being folded up completely, it forms a compact bundle. During deployment, however, the overall dimension along the solid gray guidelines increases, whereas the dimension along the broken gray guidelines reduces. A simple model of such deployable structure consisting of four large 6*R* linkages is shown in Fig. 10.

It has been noted that the bifurcation associated with a single 6*R* linkage does not appear in the assembly because some of the links obstruct the certain motion of other links during deployment.

5 Conclusions and Further Discussion

In this paper, a 5*R* linkage, named as the extended Myard linkage, is obtained by combining two Bennett linkages as Myard did in the creation of his "number 1" 5*R* linkage. The closure equa-

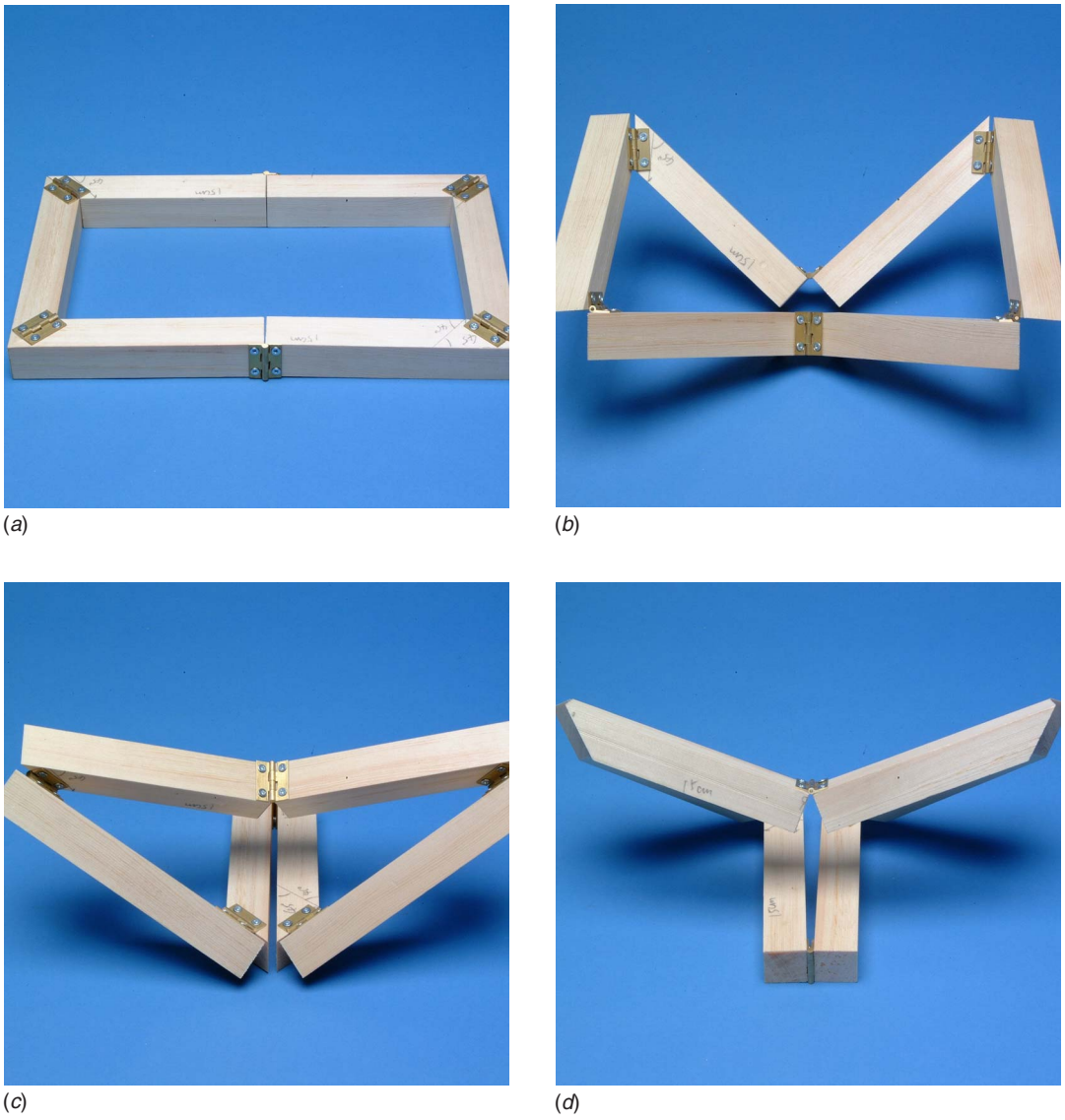

Fig. 8 Bifurcations of the 6*R* linkages

tions of the extended Myard linkage have been derived from the two general Bennett linkages that have two equal lengths and one identical twist and one complimentary twist. A 6*R* linkage has also been constructed by merging two extended Myard linkages with the closure equations. The 6*R* linkage can be used as a deployable unit for building large-scale deployable structures. Its characteristics of bifurcation have also been discussed.

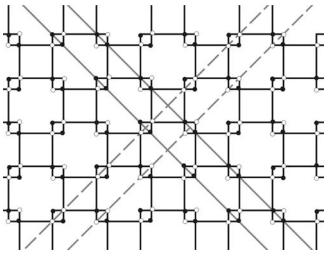

Fig. 9 A schematic diagram for an assembly of the new 6*R* linkages

Both Wohlhart [7] and Baker [11] showed that Myard's number 1 linkage is a special case of the generalized Goldberg 5*R* linkage. It can be shown that the same is true with the extended Myard linkage. Hence, the closure equations for both Myard and extended Myard linkages can be derived from those of the generalized Goldberg 5*R* linkage. Moreover, the newly found 6*R* linkage is also a special case of the Wholhart hybrid 6*R* linkage obtained by merging two generalized Goldberg 5*R* linkages because the extended Myard linkage is a special case of it.

Note that all of the offsets of both extended Myard linkage and 6*R* linkage have been set to be zero. Baker [10] showed that the Myard linkage could have nonzero offset for Joints 1, 2, and 5, see Fig. 1. Further study is necessary to examine whether the same applies to the extended Myard linkage.

A further note of interest is that the new 6*R* linkage with $\alpha_{12} = \alpha_{56} = \pi/2$ and $\zeta = \pi/2$ can also be regarded as a special case of Altman linkage [17].

Finally, from a practical perspective, the shortcoming of this 6*R* linkage as a deployable building block is that it can only fold in one direction while the dimension in another direction reaches its maximum. This problem may be solved by adopting alternative forms as we did with the Bennett linkages [18,19].

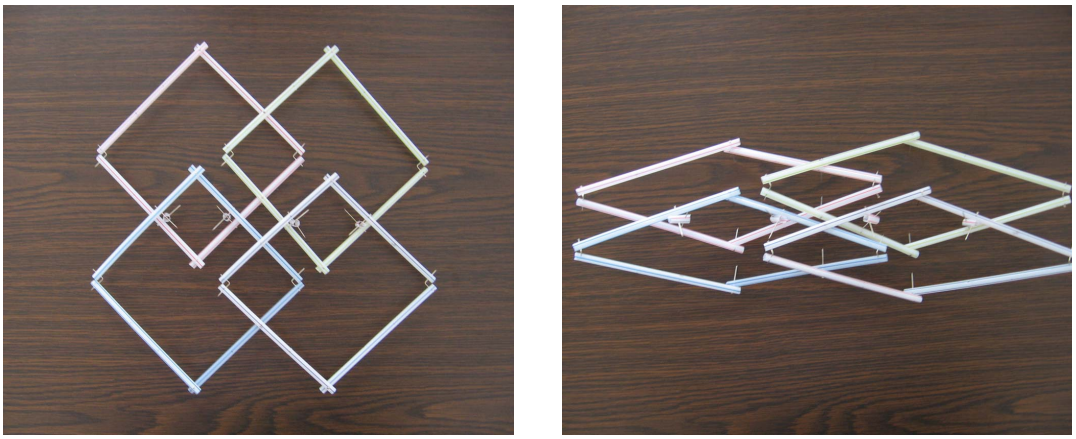

(*a*) (*b*)

(*c*)

Fig. 10 ((*a*) and (*b*)) **A deployable model consisted of four large 6*R* linkages in two different configurations.** (*c*) **The model is deployed by extending in one direction.**

Acknowledgment

Y.C. would like to thank Nanyang Technological University, Singapore, for providing a research grant (RG21/05) and granting subsequent academic leave to undertake works related to this paper. Z.Y. acknowledges with thanks financial support from the Engineering and Physical Sciences Research Council of the UK (Research Grant: EP/E502903).

Nomenclature

$a_{1,2},\ldots$ = the length of a link as the distance between the axes of two neighboring revolutes 1, 2, etc.

a, b = constants for the length of the links

a, **b**, **c**, and **d** = the superscripts to represent Bennett linkages **a**, **b**, **c**, and **d**

e and **f** = the superscripts to represent extended Myard 5*R* linkages **e** and **f**

g and **h** = the superscripts to represent the 6*R* linkages **g** and **h**

K = constant in the closure equations for the Bennett linkages

m = the superscript to represent Bennett linkages

$R_1, R_2,\ldots$ = the offsets at revolutes 1, 2, etc.

$\alpha_{1,2},\ldots$ = the twist of a link, which is defined as the skewed angle between the axes of two neighboring revolute Joints 1, 2, etc.

α, β, ζ = constants used to represent the skewed angles between the axes of two adjacent revolute joints

$\varphi_1,\ldots$ = the revolute variable at Joint 1, etc., for the extended Myard 5*R* linkage

$\mu_1,\ldots$ = the revolute variable at Joint 1, etc., for the proposed 6*R* linkage

$\theta_1,\ldots$ = the revolute variable at Joint 1, etc., for the Bennett linkage

References

[1] Hunt, K. H., 1978, *Kinematic Geometry of Mechanisms*, Oxford University Press, Oxford.

[2] Bennett, G. T., 1903, "A New Mechanism," Engineering (London), **76**, pp. 777–778.

[3] Myard, F. E., 1931, "Contribution à la Géométrie des Systèmes Articulés," Bulletin de la Société Mathématique de France, **59**, pp. 183–210.

[4] Goldberg, M., 1943, "New Five-Bar and Six-Bar Linkages in Three Dimensions," Trans. ASME, **65**, pp. 649–663.

[5] Mavroidis, C., and Roth, B., 1994, "Analysis and Synthesis of Overconstrained Mechanism," *Proceedings of the 1994 ASME Design Technical Conference*, Minneapolis, MI, Sept., pp. 115–133.

[6] Dietmaier, P., 1995, "A New 6*R* Space Mechanism," *Proceedings of the Ninth World Congress IFToMM*, Milano, Vol. 1, pp. 52–56.

[7] Wohlhart, K., 1991, "Merging Two General Goldberg 5*R* Linkages to Obtain a New 6*R* Space Mechanism," Mech. Mach. Theory, **26**(2), pp. 659–668.

[8] Chen, Y., 2003, "Design of Structural Mechanism," Ph.D. thesis, University of Oxford.

[9] Baker, J. E., 2006, "On Generating a Class of Foldable Six-Bar Spatial Linkages," ASME J. Mech. Des., **128**, pp. 374–383.

[10] Baker, J. E., 1979, "The Bennett, Goldberg and Myard Linkages—in Perspective," Mech. Mach. Theory, **14**, pp. 239–253.
[11] Baker, J. E., 1993, "A Comparative Survey of the Bennett-Based 6-Revolute Kinematic Loops," Mech. Mach. Theory, **28**, pp. 83–96.
[12] Gan, W. W., and Pellegrino, S., 2003, "Closed-Loop Deployable Structures," *Proceedings of the 44th AIAA/ASME/ASCE/AHS/ASC Structures, Structural Dynamics and Materials Conference*, Norfolk, VA, Apr. 7–10, AIAA Paper No. 2003-1450.
[13] Briand, S., and You, Z., 2007, "New Deployable Mechanisms," Department of Engineering Science, University of Oxford, Report No. 2293/07.
[14] Calladine, C. R., 1978, "Buckminster Fuller's "Tensegrity" Structures and Clerk Maxwell's Rules for the Construction of Stiff Frames," Int. J. Solids Struct., **14**, pp. 161–172.
[15] Calladine, C. R., and Pellegrino, S., 1991, "First-Order Infinitesimal Mechanisms," Int. J. Solids Struct., **27**(4), pp. 505–515.
[16] Chen, Y., You, Z., and Tarnai, T., 2005, "Threefold-Symmetric Bricard Linkages for Deployable Structures," Int. J. Solids Struct., **42**(8), pp. 2287–2301.
[17] Altmann, P. G., 1954, "Link Mechanisms in Modern Kinematics," Proc. Inst. Mech. Eng., **168**(37), pp. 889–896.
[18] Chen, Y., and You, Z., 2006, "Square Deployable Frame for Space Applications: Part I: Theory," Proc. Inst. Mech. Engr., Part G: J. Aerosp. Eng., **220**(4), pp. 347–354.
[19] Chen, Y., and You, Z., 2007, "Square Deployable Frame for Space Applications: Part II: Realisation," Proc. Inst. Mech. Engr., Part G: J. Aerosp. Eng., **221**(1), pp. 37–45.